◆ Human Brain Mapping 35:5962–5973 (2014) ◆

Sequential Evolution of Cortical Activity and Effective Connectivity of Swallowing Using fMRI

Paul Glad Mihai,[1]* Mareile Otto,[2] Thomas Platz,[2] Simon B. Eickhoff,[3,4] and Martin Lotze[1]

[1]*Functional Imaging Unit, Department of Diagnostic Radiology and Neuroradiology, Ernst-Moritz-Arndt-Universität, Greifswald, Germany*
[2]*BDH-Klinik Greifswald, Neurorehabilitation Centre and Spinal Cord Injury Unit, Neuroscience Department, Ernst-Moritz-Arndt-Universität, Greifswald, Germany*
[3]*Institute for Clinical Neuroscience and Medical Psychology, Heinrich-Heine Universität Düsseldorf, Düsseldorf, Germany*
[4]*Institute of Neuroscience and Medicine (INM-1), Research Center Jülich, D-52425 Jülich, Germany*

Abstract: Swallowing consists of a hierarchical sequence of primary motor and somatosensory processes. The temporal interplay of different phases is complex and clinical disturbances frequent. Of interest was the temporal interaction of the swallowing network. Time resolution optimized functional magnetic resonance imaging was used to describe the temporal sequence of representation sites of swallowing and their functional connectivity. Sixteen young healthy volunteers were investigated who swallowed 2 ml of water 20 times per run with a repetition time for functional imaging of 514 ms. After applying the general linear model approach to identify activation magnitude in preselected regions of interest repeated measures analysis of variance (rmANOVA) was used to detect relevant effects on lateralization, time, and onset. Furthermore, dynamic causal modeling (DCM) was applied to uncover where the input enters the model and the way in which the cortical regions are connected. The temporal analysis revealed a successive activation starting at the premotor cortex, supplementary motor area (SMA), and bilateral thalamus, followed by the primary sensorimotor cortex, the posterior insula, and cerebellum and culminating with activation in the pons shortly before subsiding. The rmANOVA revealed that activation was lateralized initially to the left hemisphere and gradually moved to the right hemisphere over time. The group random effects DCM analysis resulted in a most likely model that consisted of inputs to SMA and M1S1, bidirectionally connected, and a one-way connection from M1S1 to the posterior insula. *Hum Brain Mapp 35:5962–5973, 2014.* © 2014 Wiley Periodicals, Inc.

Key words: swallowing; functional magnetic resonance imaging; dynamic causal modeling; high temporal resolution; event related

This article was published online on 17 July 2014. An error was subsequently identified. This notice is included in the online and print versions to indicate that both have been corrected on 25 July 2014.
Contract grant sponsor: Deutsche Forschungsgemeinschaft (DFG); Contract grant number: LO 795-12; Contract grant sponsor: National Institute of Health Grants (to S.B.E.); Contract grant number: R01-MH074457-01A1; Contract grant sponsor: Deutsche Forschungsgemeinschaft [DFG (to S.B.E.)]; Contract grant numbers: EI 816/4-1, LA 3071/3-1; Contract grant sponsor: Helmholtz Initiative on Systems Biology (to S.B.E.); Contract grant sponsor: European EFT Program [Human Brain Project (to S.B.E.)].

*Correspondence to: P. G. Mihai; Functional Imaging Unit, Department of Diagnostic Radiology and Neuroradiology, Ernst-Moritz-Arndt-Universität, 17475 Greifswald, Germany.
E-mail: mihaip@uni-greifswald.de

Received for publication 22 January 2013; Revised 2 July 2014; Accepted 14 July 2014.
DOI: 10.1002/hbm.22597
Published online 17 July 2014 in Wiley Online Library (wileyonlinelibrary.com).

INTRODUCTION

Swallowing consists of a combination of well-timed sensory and motor functions working together to safely and easily transport saliva or ingested material from the mouth to the stomach [Dodds, 1989]. It is divided into three phases: oral, pharyngeal, and esophageal. Both the pharyngeal and esophageal phases are involuntarily controlled [Dodds, 1989; Jean, 2001].

The functional representation of swallowing is widely investigated and the following representational sites have been described: bilateral inferior precentral and postcentral gyri [Malandraki et al., 2009; Toogood et al., 2005], bilateral anterior insula [Humbert et al., 2009; Humbert and Robbins, 2007; Mihai et al., 2013; Riecker et al., 2009], anterior cingulate cortex [Toogood et al., 2005], bilateral temporal pole, and supplementary motor area (SMA) [Hamdy et al., 1999; Mihai et al., 2013; Mosier and Bereznaya, 2001]. A study on monkeys [Arce et al., 2013] has shown that orofacial primary motor and somatosensory cortices are highly involved in the direction of tongue protrusion, which in turn is of great importance for proper bolus control during swallowing. Two reviews [Humbert and Robbins, 2007; Michou and Hamdy, 2009] and a meta-analysis [Sörös et al., 2009] describe that the SMA, the primary motor (M1) and sensory (S1) cortex, the anterior cingulate cortex, and insular cortex are consistently active during swallowing in human brain imaging studies. Additionally, lateralization is seen in the left hemisphere during the planning stage of swallowing and in the right hemisphere during execution of the task in young healthy volunteers [Malandraki et al., 2010]. Furlong et al. [2004] have shown in a magnetoencephalography (MEG) study that there is a temporal synchrony relating the sensory and motor cortices during volitional swallowing. Water infusion activates the caudolateral sensorimotor cortex which is said to prime the swallowing task and volitional swallowing and tongue movement provide a stronger activation in the superior sensorimotor cortex. Another MEG study [Dziewas et al., 2003] shows a strong lateralization to the left during volitional swallowing with activation in the midlateral primary sensorimotor cortex and less left lateralization during reflexive swallowing. In a more time-resolved analysis, a lateralization corresponding to the early swallowing stage in the left hemisphere which gradually shifts to the right hemisphere during later stages has been recently reported [Teismann et al., 2009]. Nevertheless, the spatial resolution of MEG is limited and best identification of dipoles is only possible close to the scalp. Thus, time-dependent activation during swallowing among the consistently active regions in functional magnetic resonance imaging (fMRI) experiments is still open to questions on how they are connected and what their temporal progression is.

Dynamic causal modeling (DCM) models interactions between neuronal populations and is based on hemodynamic time series. It aims to estimate and make inferences about the coupling among brain areas and how this coupling is influenced by experimental context [Friston et al., 2003]. In this study, DCM was used to make inferences about the coupling among regions during swallowing and where the direct influence enters the model.

The aim of this study was to investigate changes in activation over time during a water swallowing task in young healthy subjects. The swallowing task was cued visually by a color change, which indicated the 2-ml water infusion. Examining the statistical parametric maps of activated regions over time, consecutive activation patterns are expected: starting from the premotor and SMAs relating to the preparation of the task, continuing on to the somatosensory cortex, cerebellum, and posterior insula where conscious action of swallowing takes place and ending with activation in the brainstem, alongside cortical activation, in line with peristalsis [Goyal and Chaudhury, 2008]. Repeated measures analysis of variance (rmANOVA) was used to find significant effects on lateralization over time, time effect for each region, and onset effect between regions. With DCM, the effective connectivity between SMA, M1S1, and the posterior insula was investigated. It was postulated that the motor planning in the SMA receives the information over the on-screen color change, that is, the instructions to prepare the swallowing task, from the visual cortex (not covered in the scanning volume). Further, the sensory input from the liquid in S1 may also contribute to planning and executing the swallow. The information could then be passed on to the posterior insula, which mediates the task.

METHODS

Participants

Sixteen neurologically healthy volunteers [average age: 24.9 ± 3.5 year (means $\pm$ standard deviation); range: 20–33 years, 11 female] were analyzed in the study in return for monetary compensation. Informed, written consent was obtained from each participant. Subjects were asked for medication status, signs of chronic pain, sensory deficits, motor deficits, epilepsy, or problems with swallowing. No participant reported to have a history of these symptoms. Three female participants indicated use of an oral contraceptive, one of which also used iron supplements. Three of the sixteen subjects reported to be left handed.

All procedures were approved by the Ethics Committee of the Medical Faculty of the University of Greifswald (registration number BB 101/08).

Procedure

Swallowing was recorded in three different runs: two functional and one MRI movie sequence. For each of the two functional runs (one using a slow repetition time (TR) of 2 s [slow echo planar image (EPI)], another using a fast

TR of 514 ms (fast EPI)), 20 swallows were recorded per run with a stimulus onset asynchrony (SOA) of 11 scans for slow EPI and 22 scans for fast EPI. For the MRI movie sequence, subjects had to swallow 10 times with a SOA of 6.1 s. The room temperature water (2 ml, injection velocity 2 ml/s) was delivered through a soft rubber tube (diameter: 1.5 mm), held between the subject's lips at midline, using a MR-safe contrast agent injector (Spectris Solaris; Medrad, Warrendale, PA). Water was used because it does not provide a high degree of swallowing difficulty compared to saliva. A thicker fluid reduces the swallowing difficulty further [Humbert et al., 2009], yet the choice of water was based on its universally reliable viscosity at room temperature ensuring reproducibility among and across experiments. Water delivery was marked by a cued color change (blue: rest, green: water injection) projected onto a translucent screen placed inside the scanner bore. The green light lasted for one scan for the slow TR measurement and two scans for the fast TR measurement. Subjects were instructed to swallow right after complete arrival of water (1 s after color change/water injection) and to avoid swallowing in between water delivery. According to a Go-No-Go swallowing experiment [Toogood et al., 2005] areas most significantly related to the No-Go task were restricted to the cuneus and precuneus, whereas precentral and postcentral gyri, together with the anterior cingulate cortex show a significantly greater activation related to the Go swallowing task. Hence, the influence of the instruction to avoid swallowing between water deliveries, which can be interpreted as a No-Go task, is not related to motor and somatosensory activation. Swallowing timing and task compliance was controlled using a pneumatic cushion attached to the neck of the subject. Thyroid cartilage movement exerts a pressure on the cushion during the swallowing task. The change in air pressure from the cushion is transformed by a pressure detector into an electrical signal measured by an electro-optical biosignal recorder (Varioport-b; Becker meditec, Karlsruhe, Germany). The pressure was used as a reference to determine individual starting times for oral and pharyngeal stages of swallowing. Even though thyroid cartilage movement can reflect oropharyngeal movement in the absence of a pharyngeal swallow, subjects were clearly and repeatedly instructed to swallow once after each water delivery. It is highly unlikely that subjects would have raised the thyroid cartilage without a proceeding swallow, shortly after water delivery.

Data Acquisition and Processing

MRI data acquisition was performed on a 3 T MRI scanner (Siemens Verio, Erlangen, Germany) using a 32-channel head coil. Two functional event-related imaging runs (one fast, one slow), an MRI movie sequence, and a T1-weighted high resolution whole head dataset were recorded in one experimental session. Field homogeneity was optimized by a shimming sequence and a gradient echo sequence (34 phase and magnitude images, 7 slices, 3 $\times$ 3 $\times$ 4 mm^3, field of view (FoV) 192 mm, TR 488 ms, TE_1 4.92 ms, TE_2 7.38 ms, $\alpha = 60°$) was acquired to calculate a field map aiming at correcting geometric distortions in the EPI. Fast functional EPI (TR 514 ms, TE 30 ms, $\alpha = 90°$, FoV 192 mm, voxel size 3 $\times$ 3 $\times$ 4 mm^3, distance factor 50%, base resolution 64 $\times$ 64, oblique orientation, 464 volumes, interleaved) consisted of seven slices in order to increase the temporal resolution of image acquisition for a more precise sampling of the blood oxygen level dependent (BOLD) signal. In addition, our experience in artifact reduction suggested the usage of slice orientation parallel to the central sulcus. This was a tradeoff between high temporal resolution and volume covered with the focus on the main sensorimotor areas. Unfortunately, areas such as the anterior cingulate cortex which has been shown to be consistently involved in swallowing [Humbert and Robbins, 2007; Michou and Hamdy, 2009; Sörös et al., 2009] could not be included. These slices encompass the brain areas involved in sensorimotor processing, posterior insula, and parts of the cerebellum and brainstem as shown in Figure 1a. Stereotaxic coordinates for the relevant anatomic regions encompassed by these slices are found in Table I. Slow functional EPI [Mihai et al., 2013] were the basis for the functional localizer of swallowing. The cinematographic (CINE) sequence (cardio vascular imaging sequence, TR 2.7 ms, TE 1.22 ms, $\alpha = 50°$, FoV 270 mm, voxel size 2.8 $\times$ 2.8 $\times$ 10 mm, parallel acquisition using a *k*-space-based algorithm [GRAPPA] factor 2, distance factor 10%, base resolution 96 $\times$ 96, sagittal orientation, 1 slice, 200 volumes) was used to visualize the movement of water, tongue, and pharynx during 10 swallowing trials. The effective TR was 305 ms which resulted in a frame rate of 3.3 frames per second. In addition, a T1-weighted anatomical image was acquired (magnetization-prepared rapid gradient echo, TR 1690 ms, TE 2.52 ms, $\alpha = 9°$, FoV 250 mm, voxel size 1 $\times$ 1 $\times$ 1 mm^3, parallel acquisition using a *k*-space-based algorithm [GRAPPA] factor 2, matrix 256 $\times$ 256, distance factor 50%, transversal orientation, 176 slices, ascending).

Color changes were triggered with fMRI scans, which in turn sent trigger signals to the pressure recorder. This ensured that all data acquisition modalities were synchronized, and allowed for exact timing of thyroid cartilage movement relative to light change.

The cinematographic imaging data were analyzed by a speech-language pathologist (MO) to distinguish the time points of oral and pharyngeal phases for each subject. The beginning of the oral and pharyngeal phases was marked relative to the thyroid cartilage movement by visual inspection of the CINE images. Individual average outset times of the oral and pharyngeal phases were thus obtained.

Preprocessing of fMRI data was done in SPM8 rev. 5236 (Wellcome Department of Imaging Neuroscience, London, UK) running on MATLAB R2011a (MathWorks, Natick,

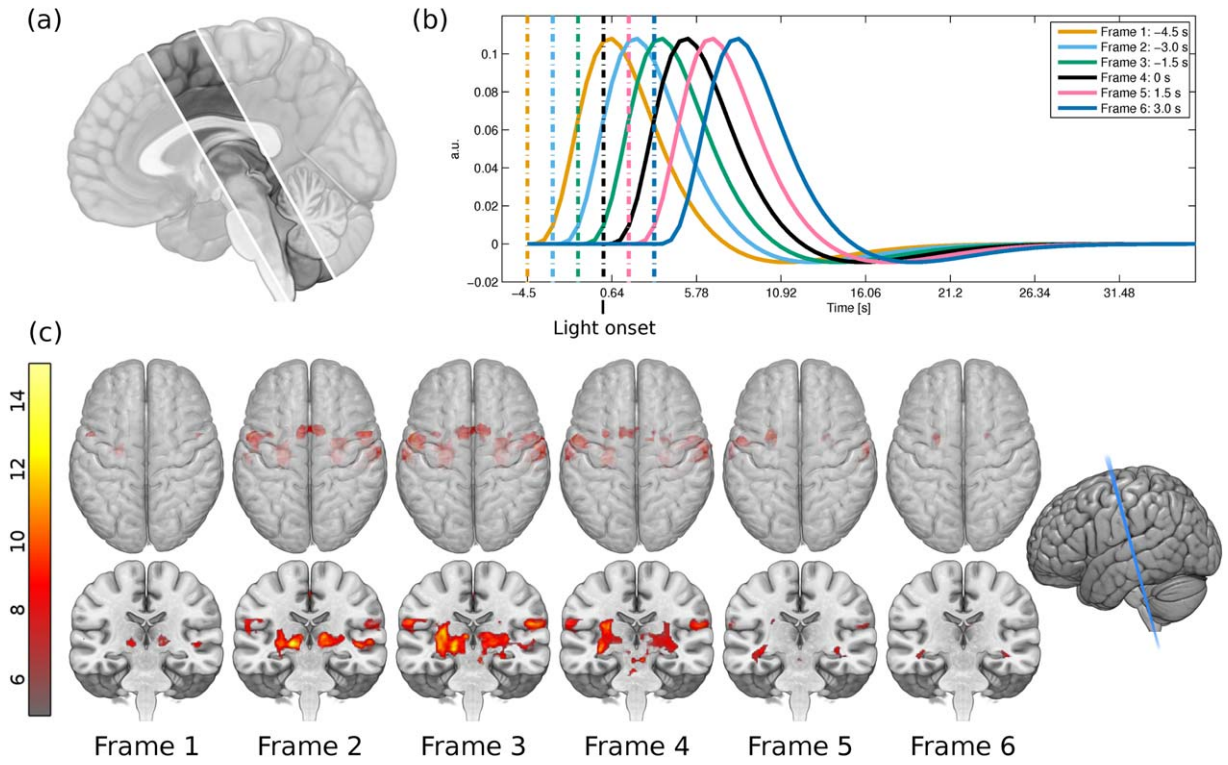

Figure 1.

(**a**) Only seven slices were recorded in the fast EPI measurement, which limited the scanned volume to slices encompassing the PMC, SMA, M1, S1, S2, posterior insula, cerebellum, and brainstem. This image is a graphical representation of the brain covered by the seven slices; the faded parts were not included in the measurement. (**b**) A plot of the six different HRFs used in the GLM analysis, named Frame 1 through Frame 6 from left to right. Frame 4 represents the light onset. The interrupted lines represent the onset times while the solid lines represent the corresponding HRFs. (**c**) Statistical parametric maps for the six HRFs used in the GLM analysis. The top row shows the axial view with the rendering made translucent, so that deeper activations can be seen. The bottom row shows a coronal cut, slightly oblique as depicted on the far right. The color bar depicts the *t*-score from gray (lowest) to bright yellow (highest). [Color figure can be viewed in the online issue, which is available at wileyonlinelibrary.com.]

MA). Every swallow causes head movement which is correlated with the stimulus. Movement parameters from a first realignment procedure were used to assess these motion artifacts which were removed with the help of the ArtRepair Toolbox [Mazaika et al., 2009] by interpolating between the adjacent data points. Movement reduced data were processed as follows. Images were slice time corrected to the middle slice using SPM8's Fourier phase shift interpolation. Head motion was corrected with SPM8's Realign and Unwarp via a third degree b-spline interpolation using the first scan of the series as reference. Unwarping of susceptibility by movement interaction was done with the help of a voxel displacement map calculated from the field map data. Each subject's T1 image was coregistered using the normalized mutual information from the last step to the mean EPI image. T1 images were segmented into gray and white matter maps using the modified International Consortium for Human Brain Mapping (ICBM) tissue probability maps in Montreal Neurological Institute (MNI) space provided by SPM8. EPI were normalized to the ICBM 152 nonlinear MNI template using a trilinear interpolation. A 6 × 6 × 6 mm^3

TABLE I. Stereotaxic coordinates of analyzed regions

	MNI coordinates		
Region	*x*	*y*	*z*
M1S1 L	−56	−5	−24
M1S1 R	60	−5	23
SMA	2	9	52
Posterior Insula L	−34	−14	12
Posterior Insula R	37	−14	11
Cerebellum L	−14	−33	−23
Cerebellum R	17	−33	−22

Stereotaxic coordinates for central points where there is an overlap between slice coverage and anatomical regions. L: left, R: right.

full-width at half-maximum Gaussian kernel filter was used to increase the signal-to-noise ratio and reduce intersubject differences.

Three methods were used to statistically analyze the fast functional data. The first used the general linear model (GLM) implemented in SPM8. rmANOVA was used to find significant interactions for region, side, and time. Lastly, effective connectivity of the regions involved in swallowing was examined.

GLM Analysis

For the first method within subject, first-level analysis was performed using the GLM implemented in SPM8. Low frequency components were filtered with a high-pass filter having a cutoff of 128 s, or 0.008 Hz. SPM's canonical hemodynamic response function (HRF) was used as the model for the BOLD response. Motion parameters from the realignment procedure of the artifact repaired data were used as covariates in the design matrix. The autocorrelation inherent in the data was estimated by an autoregressive AR(1) model.

Hüslmann et al. [2003] used a self-paced task involving a random button press in a specific time interval to reveal a sequential activation in the anterior cingulate cortex through the SMA and premotor area to the primary motor (M1) and somatosensory (S1) cortex. Under assumption of the canonical HRF, the voxelwise calculation of maps prior and following the self-paced movement were analyzed. A partially comparable approach was used here. GLMs and contrasts of interest were calculated for swallowing versus baseline at six different onset times in steps of 1.5 s from −4.5 to 3.0 s with time 0 s being the light change from blue to green (Fig. 1b), that is, water injection time. The six onset times when convolved with the HRF cover an epoch that spans the expected BOLD responses initiated by swallowing. The choice of time windows was based on the analysis of the BOLD signal relative to the color change onset. Figure 2 shows a plot of the pressure cushion signal aligned with the BOLD response in M1S1 and compared with the theoretical HRF based on two different onsets. The onsets corresponded to the color change (interrupted blue vertical line) and to the approximate peak of the pressure signal from laryngeal movement (solid red, vertical line). The resulting HRFs (onset times convolved with canonical HRF) clearly showed that they are in agreement with the color change onset. The pressure signal onset results in a later HRF which is not mirrored in the measured signal. A GLM was calculated per time frame for each subject. These steps were chosen empirically in order to accommodate for significant changes between intervals. Smaller steps resulted in fewer changes from one frame to the next. Temporal derivatives were not included in the design matrix as they are only reliable for ±1 s [Friston et al., 2007]. A random effects inference was done with a one sample *t*-test on the summary statistic per contrast of each time frame. Location of activation maxima for all time points were recorded in a table with the help of anatomical masks obtained from the Anatomy Toolbox [Eickhoff et al., 2005] for the SMA, PMC, and M1S1. For the differentiation of the PMC and the SMA, which are cytoarchitectonically similar, a spatial differentiation was performed: the PMC was defined as the BA 6 lateral to the superior frontal sulcus of the MNI-template ($-30 < x > 30$). Cerebellar maps, comprising Larsell's classification IV–VI (culmen and declive), insula, and pons were obtained from the WFU PickAtlas [Maldjian et al., 2003].

Repeated Measures Analysis of Variance

A repeated measures analysis of variance (rmANOVA) was calculated for the beta-values averaged in a 6-mm sphere around the highest activated voxel within each regions of interest (ROI) used in the GLM analysis for the factors: region (PMC, SMA, M1S1, posterior insula, and cerebellum), side (left and right), and time (Frames 1, 2, 3, 4, 5, 6). The Greenhouse-Geisser correction was used for detecting significant main effects and interactions. Significant effects in rmANOVA were followed by the following post hoc *t*-tests, based on our hypotheses and the results from previous studies:

1. Lateralization effect over time for three time frames: Frame 2, Frame 3, and Frame 6 (three comparisons per region; $p_{corr} = 0.016$);
2. Time effect for each region (averaged for side; six comparisons; $p_{corr} = 0.008$);
3. Onset effect between regions (averaged for side; five comparisons; $p_{corr} = 0.01$).

Dynamic Causal Modeling

The second method dealt with effective connectivity and used DCM [Friston et al., 2003] as implemented in SPM8 (DCM10 for SPM8). DCM models interactions at the cortical level using hemodynamic time series. It aims to estimate and make inferences about coupling among brain regions and how this coupling is influenced by changes in experimental contexts.

DCM's purpose in this experiment was two-fold. First, what was the role of the input, especially as there are two possible cues to plan and execute swallowing—visual and somatosensory? Second, based on these cues, what is the directionality of the connections during motor planning, motor execution, and mediation? Models were based on simplicity and focused on three seeds. These included the SMA, used in planning and execution stages of complex motor movements such as swallowing [Hamdy et al., 1999; Mosier and Bereznaya, 2001]. The primary sensorimotor cortex (M1S1) plays an important role on muscle control and sensory feedback during swallowing [Malandraki et al., 2009]. M1 and S1 were grouped together as M1S1 due to low spatial resolution and smoothing, smearing activation in such a small volume. Lastly, the insula was included

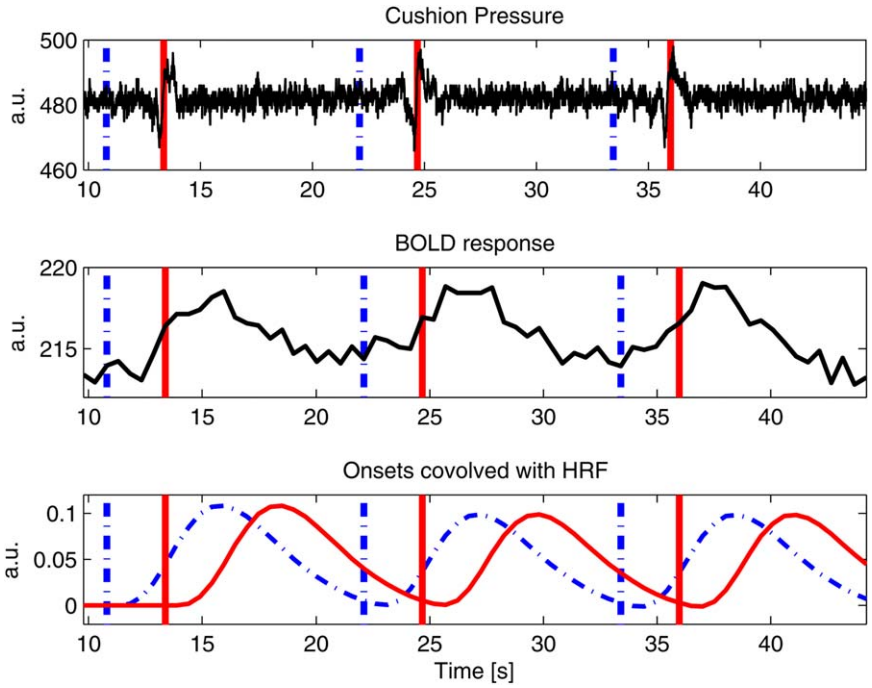

Figure 2.

A plot illustrating the pressure cushion signal, BOLD response from the highest activated voxel in M1S1 for a representative subject and onsets convolved with the HRF, plotted against time. All three plots are synchronized in time. Vertical lines indicate onset times for color change (interrupted line) and thyroid cartilage movement (solid line). The HRF aligned with color change (interrupted line) properly corresponds with the BOLD response, as opposed to the HRF aligned with thyroid cartilage movement (solid line). [Color figure can be viewed in the online issue, which is available at wileyonlinelibrary.com.]

which has connections to primary and supplementary motor cortices and is key in mediation of oropharyngeal swallowing [Daniels and Foundas, 1997]. The limitation to three regions was introduced to reduce the complexity of the models and to gather information on which input is used as a cue to swallow, where it enters the model and how these three regions interact given this input. Furthermore, the seven slices limited the full coverage of the regions. Left and right hemispheres were analyzed separately, save for the SMA due to its central location and short pathways between hemispheres.

Seed regions for DCM computation were made using a combination of functional ROI and the Anatomy Toolbox for SPM8 [Eickhoff et al., 2005] as well as the WFU PickAtlas [Maldjian et al., 2003]. The functional ROIs were extracted from the EPI data recorded with a TR of 2 s (slow EPI). This data had 34 slices and thus a larger volume providing better coverage. The slow EPI experiment also showed activation for the three seed ROI in the DCM analysis [Mihai et al., 2013]. The functional ROI was masked by the probabilistic ROIs from the Anatomy Toolbox which included masks for the SMA (combined left and right hemisphere due to the short connections between the hemispheres, BA 6), M1S1 (left and right hemisphere, BA 4a, 4p, 3a, 3s, 1, 2). The insula (left and right hemisphere) was provided by the WFU PickAtlas [Maldjian et al., 2003]. A representative time course from voxel data in terms of the first eigenvariate in all suprathreshold voxels ($P < 0.05$ FWE corrected) in the fast EPI data was extracted using the combined ROIs for each subject.

Model Selection and Comparison

Figure 3 shows the models. For model (a), the stimulus information enters the SMA which is connected directionally to M1S1. The idea here is that color change marking the time of water infusion through the visual cortex induces a preparatory activation in the SMA. Model (b) connects both SMA and M1S1 bidirectionally while the input enters M1S1. Here, the water entering the mouth stimulates S1, which sends the signal to the SMA, inducing swallowing action through M1. Model (c) is based on (b) with the exception that the input reaches both the SMA as a visual input and M1S1 as a sensory input. All models have a one-way connection from M1S1 to the posterior insula. The unidirectional connection from M1S1 to the anterior insula was chosen because it has been suggested that the function of the posterior insula lays predominantly in monitoring body states and integrating

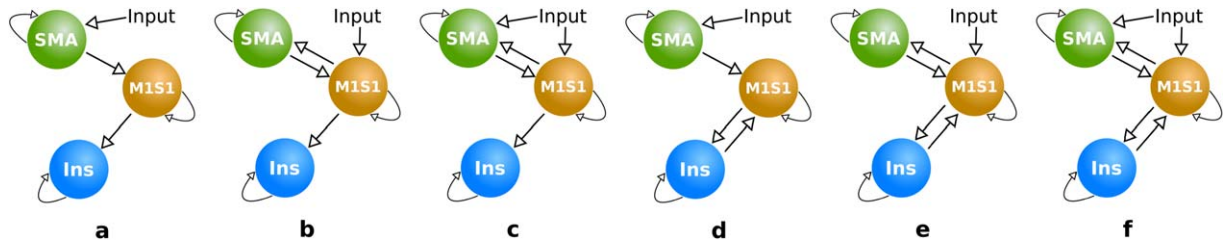

Figure 3.

Description of the models used to test the effective connectivity of the regions. Model (a) receives the input at the SMA, which is connected unidirectionally to M1S1. Model (b) receives the input at M1S1; both regions are connected bidirectionally. Model (c) has inputs going to both the SMA and M1S1; both regions are connected bidirectionally. All models have a one-way connection from M1S1 to the posterior insula. Models (d) through (f) are similar to models (a) through (c), with the exception of a bidirectional connection between M1S1 and insula. [Color figure can be viewed in the online issue, which is available at wileyonlinelibrary.com.]

somatosensory input to this state [Damasio, 1996]. Therefore, the direction of the model should be unidirectional from the sensorimotor system to the posterior insula. However, to test the influence of the bidirectional connection between M1S1 and posterior insula, three additional models [Fig. 3 models (d), (e), and (f)] were added. These were based on the first three, with an affixed connection from anterior insula to M1S1.

The six models were specified, estimated, and compared at the group level.

To identify the most likely generative model for the observed data among the six different models, a random-effects Bayesian Model Selection (BMS) procedure was employed [Stephan et al., 2009] where all models were tested against each other. This Bayesian method treats the model as a random variable and estimates the parameter of a Dirichlet distribution, which describes the probabilities for all models being considered and allows computing the exceedance probability of one model being more likely than any other model tested.

RESULTS

All results reported here are based on the fast EPI data (TR = 514 ms).

Task Performance

The swallowing task was verified with the help of the pneumatic cushion measurements. All subjects swallowed 20 times except for two, each omitting one swallow. This was accounted for in the analysis. The mean (± standard deviation) time difference across subjects from color change to pressure cushion signal was 2.8 ± 0.6 s.

GLM Analysis

The evolution of BOLD activity over time as calculated by the GLM analysis is depicted in Figure 1c. At the first time frame, cortical activation was exhibited in the left posterior SMA and premotor cortex (PMC) in the somatotopic height of lip and tongue and subcortical bilateral thalamus. In Frame 2, the bilateral anterior and posterior SMA and PMC were activated, primary motor (M1) activation was detected, and the bilateral thalamus was active. In Frame 3, activation magnitude was highest for all areas described including bilateral primary and secondary somatosensory cortex (S1 and S2) but also bilateral posterior insula. Activation difference was minimal in the BOLD magnitude of the following time frame (Frame 4; light change/water injection time), compared to the current one, with the exception of the brainstem activation. The next time frame only showed residual cortical activation in the left SMA and left M1/S1. The last frame (Frame 6) showed no significant activation magnitude. Activation maxima for all time points using anatomical maps of the PMC, SMA, M1S1, posterior insula, cerebellum, and brainstem can be found in Table II.

No significant (FWE, $P < 0.05$) activation was found for the individual average outset times of the oral and pharyngeal phases as calculated from the cinematographic images. The clarification of this result is given in Discussion Section.

Repeated Measures Analysis of Variance

Repeated measures ANOVA (rmANOVA) revealed a significant main effect for region (PMC, SMA, M1S1, posterior insula, cerebellum; $F(4, 60) = 81.92$; $P < 0.001$), time (six time frames; $F(5, 75) = 8.17$; $P < 0.01$) and a significant interaction for region x time ($F(20, 300) = 15.93$; $P < 0.001$), side × time ($F(5, 75) = 37.40$; $P < 0.01$) and region × side × time ($F(20, 300) = 4.30$; $P < 0.01$). Post hoc t-tests showed a significant lateralization effect over time for M1S1 starting with a left lateralization in Frame 2 ($t(15) = 2.80$; $P = 0.011$) and ending with a right lateralization in Frame 6 ($t(15) = -2.94$; $P = 0.010$). For the posterior insula, a right lateralization at Frame 3 was observed ($t(15) = -2.75$; $P = 0.015$) but in other areas no significant lateralization within time frames was

TABLE II. Coordinates of highest activation in GLM analysis for all six time frames

Time frames	1				2				3				4				5				6			
Macroanatomical location	*T*	MNI coordinates			*T*	MNI coordinates			*T*	MNI coordinates			*T*	MNI coordinates			*T*	MNI coordinates			*T*	MNI coordinates		
		x	*y*	*z*		*x*	*y*	*z*		*x*	*y*	*z*		*x*	*y*	*z*		*x*	*y*	*z*		*x*	*y*	*z*
L PMC	8.61	−56	2	32	16.09	−56	2	32	14.19	−56	−2	30	14.95	−56	−2	30	10.09	−56	−2	30	—	—	—	—
R PMC	7.62	52	4	42	11.57	52	4	42	10.23	58	−2	28	8.97	58	−2	28	6.72	58	0	26	—	—	—	—
L SMA	—	—	—	—	8.82	−8	4	46	9.26	8	6	48	7.81	8	12	54	—	—	—	—	—	—	—	—
R SMA	—	—	—	—	10.47	4	8	48	8.77	−8	4	46	6.91	−8	4	46	—	—	—	—	—	—	—	—
L M1S1	—	—	—	—	9.19	−54	−2	28	15.02	−54	−2	28	15.92	−54	2	28	10.61	−54	−2	28	7.06	−64	−6	22
R M1S1	—	—	—	—	9.51	54	−4	20	12.16	58	−4	24	10.41	58	−4	24	7.93	62	−8	20	—	—	—	—
L Insula	—	—	—	—	8.14	−36	−14	2	12.68	−32	−24	6	10.44	−32	−26	4	—	—	—	—	—	—	—	—
R Insula	—	—	—	—	8.96	42	−22	−2	9.96	32	−22	6	7.93	32	−28	8	—	—	—	—	—	—	—	—
L Cerebellum	—	—	—	—	—	—	—	—	—	—	—	—	7.80	−18	−38	−26	—	—	—	—	—	—	—	—
R Cerebellum	—	—	—	—	8.07	20	−38	−24	8.57	20	−38	−22	7.56	20	−36	−28	—	—	—	—	—	—	—	—
L Pons	—	—	—	—	—	—	—	—	—	—	—	—	9.50	−4	−30	−26	—	—	—	—	—	—	—	—
R Pons	—	—	—	—	—	—	—	—	—	—	—	—	—	—	—	—	—	—	—	—	—	—	—	—

Statistical parametric mapping coordinates (Montreal Neurological Institute, *x*, *y*, *z* [mm]) and *t*-values (*T*) of the highest activated voxel for the six different HRFs used in the GLM analysis. All results are plotted for $P < 0.05$, family-wise error corrected. L, left; R, right; PMC, premotor cortex; SMA supplementary motor area; M1S1, primary sensory-motor cortex; Cerebellum, cerebellar hemisphere Larsell IV–VI.

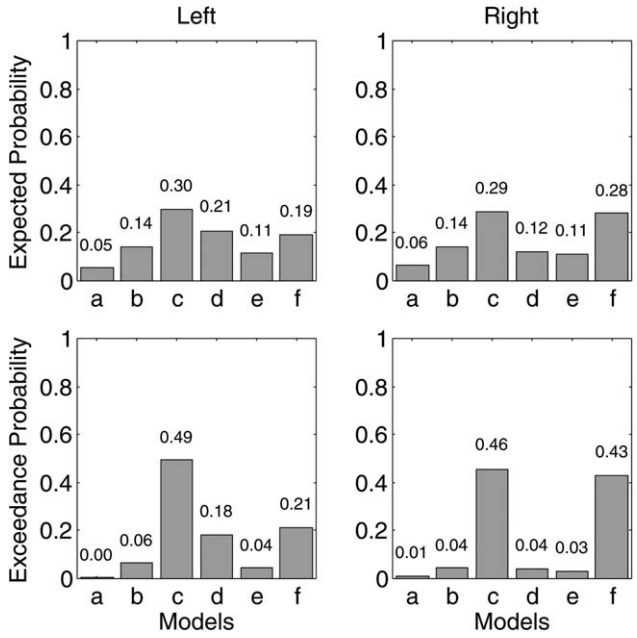

Figure 4.

Expected and exceedance probabilities for the models tested in the DCM analysis. The left column depicts the results for left hemisphere while the right column depicts the results for the right hemisphere.

present. As the side effect was not significant as a main factor, all activation magnitudes were averaged out per region and time frame for both hemispheres. When testing over time (moving *t*-tests to the prior time frame), there was a relevant increase in PMC and M1S1 from Frame 1 up to Frame 3 (Frame 1 to 6: PMC: $t(15) = -4.59$; $P < 0.001$, M1S1: $t(15) = -9.62$; $P < 0.001$; Frame 2 to 3: PMC: $t(15) = -7.55$; $P < 0.001$; M1S1: $t(15) = -5.45$; $P < 0.001$), then a plateau (M1S1 and PMC between Frames 3 and 4) and then a significant decrease (Frame 4 to 5: M1: $t(15) = 4.23$; $P < 0.001$; Frame 5 to 6 s: PMC: $t(15) = 6.61$; $P < 0.001$; M1: $t(15) = 9.21$; $P < 0.001$). In SMA, the increase seemed to be earlier (Frame 1 to 6: $t(15) = -7.06$; $P < 0.001$) and was already reversed at Frame 3 to 4 ($t(15) = 2.86$; $P < 0.012$). The increase in the posterior insula was early (Frame 1 to 2; $t(15) = -3.59$; $P < 0.003$) and was reversed already at Frame 3 to 4 ($t(15) = 3.79$; $P < 0.002$). No relevant changes were seen for the cerebellar hemisphere over time. Between the regions, there were highest BOLD-magnitudes for the PMC and M1S1 compared to SMA during the whole period between Frames 3 and 6 ($t > 5.6$; $P < 0.001$). The posterior insula showed lower BOLD magnitude during Frames 1 and 4 ($t \approx -4.2$; $P < 0.001$) followed by a comparable activation magnitude as the SMA.

Dynamic Causal Modeling

In Figure 4, the expected probability (top row) and exceedance probabilities (bottom row) of the six models tested are presented. In the left hemisphere, the winning model as computed with random effects BMS is (c) with an expected and exceedance probability of 0.30 and 0.49, respectively. In the right hemisphere, model (c) is also the winner (expected probability of 0.29, exceedance probability of 0.46) with model (f) following closely (expected probability of 0.28, exceedance probability of 0.43). Both models (c) and (f) have inputs to the SMA and M1S1 which are bidirectionally connected. The difference between the two lies in the connection to the anterior insula. Model (c) has a unidirectional connection from M1S1 to the posterior insula, while model (f) has a bidirectional connection between the two.

DISCUSSION

Cortical, cerebellar, and subcortical areas contribute to deglutition. In an attempt to discover the effective connectivity and timing between the most common activated regions during swallowing in fMRI, GLM analysis over six different time points during the task and DCM were examined in young healthy adults. In the general linear modeling analysis in time, consecutive activations were seen during swallowing starting at the PMC, SMA, and bilateral thalamus, continuing on to M1S1, insula, and cerebellum and reaching the brainstem shortly before subsiding. A rmANOVA revealed a significant activation over time in M1S1 starting in the left hemisphere and moving to the right hemisphere. The BMS of the six DCM models resulted in the most likely model having an input to both the SMA and M1S1, which were bidirectionally connected, and a one-way connection from M1S1 to the insula.

GLM Analysis

Using the GLM as implemented in SPM, statistical *t*-maps were calculated for six time points covering the whole swallowing response including the oral and pharyngeal phases. The results show a gradual increase of activation over time starting in the PMC, SMA, and bilateral thalamus, and continuing on to M1S1, posterior insula, and cerebellum. Activation in PMC and SMA were preceding movement execution and were the first sites being active for swallowing. The visual cue (color change from blue to green) was the first indicator of the task and raised awareness to prepare the swallow. Water infusion, the second cue, has been shown to activate the caudolateral sensorimotor cortex [Furlong et al., 2004]. The second frame shows starting activation in M1S1 suggesting a response to water infusion. Subcortical activation in the thalamus might have been due to a somatosensory feedback of the water pressure stimulating the tongue before the swallowing process is started. The actual execution of movement and the concomitant somatosensory processing during swallowing was expressed in the activation of M1S1, posterior insula, and cerebellum. Tongue and lips performing

the coordinated movement are guided by the sensory feedback to push the water toward the oropharynx. The activation of the pons might be indicative of the pharyngeal phase of swallowing, where the water enters the pharynx to be pushed toward the esophagus. The activation observed in the pons is consistent with the one reported in a previous study [Mihai et al., 2013] where the sensory nucleus of the trigeminal nerve and the solitary nucleus are found to be involved in the swallowing network. This study employed a lower spatial resolution and also cut out the ventral part of the brainstem when limited to only seven slices. This resulted in only one significant highest activation (coordinates: −4,−30,−26), the most likely candidate being the solitary nucleus.

Repeated Measures Analysis of Variance

The repeated measures ANOVA revealed a lateralization over time in M1S1 gradually moving from the left hemisphere (starting at Frame 1) to the right hemisphere (ending at Frame 6). Earlier stages, including the preparatory phase, were lateralized to the left and later stages were lateralized to the right hemisphere. Our findings are, therefore, consistent with the MEG findings of Teismann et al. [2009], where left hemispheric activation is found for the first 600 ms, followed by a bihemispheric activation in the next 200 ms and ending in a right hemispheric activation during the last 200 ms. The posterior insula showed a significant lateralization only at Frame 3. This may be due to its early increase and early reversal, as calculated in the region × time interaction and its comparably low activation. The SMA over time started earlier and decreased earlier corresponding to its function of readying the swallowing action. It does not explain, however, why the PMC mimics the M1S1 activation over time with a relevant increase in the early frames (Frames 1–3), a plateau (Frames 3 and 4) and a significant decrease in the latter frames. Both these regions also show a significantly higher between region activation when compared to the SMA. M1S1 activation is a reflection of the sensory-motor interaction during swallowing. The sensory aspect of the water being injected into the mouth, furthered by the swallowing action, results in a strong activation of these areas over time. The observed shift in brain activation from left to right may be associated with different specializations of cortical areas. Thus, the left hemisphere could be better specialized in the control of the preparatory phases of swallowing, while the right hemisphere may play a larger role in the involuntary phases of swallowing. This is corroborated with studies on dysphagic patients after a right hemispheric stroke. The pharyngeal phase is delayed more severely and there is a higher incidence of laryngeal penetration and aspiration in patients with right hemispheric stroke and dysphagia [Robbins, 1993]. Daniels and Foundas [1997] have shown that dysphunction and dysmotility in the pharyngeal swallowing stage were the result of right hemispheric damage. Using MEG, Dziewas et al. [2003] showed a strong lateralization to the left during volitional swallowing with activation in the midlateral primary sensorimotor cortex and less left lateralization during reflexive swallowing. Teismann et al. [2009] hypothesized that right hemispheric activation, which they have shown to occur later than left hemispheric activation, corresponds to the pharyngeal stage whereas the left hemispheric lateralization was attributed to the preparatory phase of swallowing.

DCM Analysis

The results of the DCM analysis revealed that models (c) and (f) (Fig. 3) explained the data well. Here, the SMA and M1S1 are connected bidirectionally with inputs going to both regions. The difference in models lies in the connection between M1S1 and posterior insula, with model (c) having a unidirectional connection, while model (f) a bidirectional connection. The more likely model, however, involves a unidirectional input from M1S1 to the insula [model (c)]. In the right hemisphere, models (c) and (f) have comparable exceedance probabilities, suggesting a stronger involvement of the posterior insula on M1S1 as compared to the left hemisphere. It could be argued that the posterior insula plays a greater role in the modulation of swallowing in the right hemisphere, suggesting finer involvement in later swallowing stages. The SMA most likely receives the input from the visual cortex. Due to the need for high temporal resolution, the number of slices has been reduced, omitting the visual cortex. Thus, a model involving this cortical area could not be tested. The best model also had an input to M1S1 as the primary somatosensory cortex receives information as soon as the water enters the oral cavity. The assumption that both the visual and sensory inputs play a role in this experiment is furthered by the bidirectional connection between the SMA and M1S1. The somatosensory cortex, after sensing the water entering the mouth passes this information to the SMA to prepare the motor action of swallowing. Shortly before this happens, the subject is alerted through the light change that water will soon enter the oral cavity and is thus readying the swallow. The integration of both of these cues then leads to the swallowing action performed by the motor cortex.

The DCM analysis showed that the most likely starting candidate would either be the SMA or M1S1. It cannot be discounted that both SMA and M1S1 simultaneously act as starting candidates. However, the methods outlined in this article were unable to provide a definite answer to this proposition. It can only be speculated that the visual feedback would most likely reach the cortical pathways first, as there is a reaction-time lag between color change and button-press, which results in a water injection delay relative to color change. As the infusion period is a constant for all water delivery instances, the only uncertainty factor

remains the human reaction to push the button. Nonetheless, this interruption was always in the subsecond range.

Limitations

A possible interaction of handedness and lateralization of sensorimotor representation during swallowing has been discussed before [Daniels, 2000; Dziewas et al., 2003; Hamdy et al., 1997; Kern et al., 2001; Martin et al., 2001; Mosier et al., 1999; Teismann et al., 2009]. This study did not confine the sample on right handers but used a representative one. This might have had a decreasing effect on lateralization of representation maps; yet excluding left-handed participants would have decreased the explanatory power of the study.

The study has some limitations for both the GLM and the DCM-analysis. For the GLM analysis, no significant results were found for the individual average start times of the oral and pharyngeal phases as computed from the cinematographic images. An experienced swallowing therapist, well versed in the evaluation of cinematographic data of swallowing, differentiated the onsets of these two phases. The temporal onset of the cinematographic and fMRI data was related via the pneumatic cushion which recorded thyroid cartilage movement during swallowing. Results showed no suprathreshold voxels active for the averaged onsets. However, there was a clear indication of a consecutive progression during swallowing which included these two phases when examining the activation over time. Average times from the cinematographic sequence were used for the functional calculation and there is no guarantee that the subjects performed similarly during the functional run. The cinematographic sequence used to pinpoint individual time points relating to the oral and pharyngeal phase had a temporal resolution of 305 ms (around 3.3 frames per second) comparable to pulsed fluoroscopy sequences used in low dose diagnostics (3.75 frames per second) [Stueve, 2006]. The temporal resolution affords a rough estimate of the sought out time-points which provides sufficient precision for the use as onsets in the design matrix of the GLM. The data are fitted using the canonical HRF which is fixed. Miezin et al. [2000] have shown that there is a strong amplitude reduction when using intertrial intervals of 5 s compared to longer ones. If swallow latency from the oral to the pharyngeal stage is thought to be in the range of 1 s [Ramsey, 1955; Reimers-Neils, 1994], it can be assumed that BOLD amplitudes from the pharyngeal stage are so low that they might fuse with the amplitudes of the oral stage. Hence, measured BOLD signal might contain information from both stages which may be indistinguishable with current methods. A resolution to this problem would be to differentiate the phases experimentally by instructing subjects at the first signal to move the bolus toward the pharynx, lift it, and wait for the signal to push the bolus into it. The first signal would correspond to the oral phase and the second to the pharyngeal phase. Due to the nature of the BOLD response and the way it is modeled in SPM, the timing information extracted through the GLM analysis provides limited insight and may be confusing. The activation starts at −4.5 s before light change, and thus before water injection, which is not a true reflection of the actual events. Instead, it is a result of the HRF model and its fit to the measured BOLD signal. The useful information provided by this approach is the relative sequential evolution of the cortical and subcortical activation related to the task, and not the absolute timing. In short, onset times which are thought to correspond to the oral and pharyngeal phases as calculated from the cinematographic images with the help of the thyroid cartilage movement as a reference point, do not seem to correspond to the actual time points for the swallowing stages in question of the functional images. This is furthered by the fact that BOLD responses do not correspond to thyroid cartilage movements as seen in Figure 2.

To truly differentiate the visual from the sensory input, the visual cortex should also be included in the measurement and DCM models. However, high temporal resolution at the cost of spatial coverage was a priority in this experiment. With higher field strengths and faster sequences, this may be possible in the future. Additionally, the PMC, basal ganglia, cerebellum, and pons were left out of the models to reduce complexity. The main focus of this study was the activation over time during swallowing. DCM, although not suited for timing calculations, provided a means of determining where the input enters the model and nature of directionality of the connections between regions. These results help interpret the GLM analysis.

CONCLUSIONS

The GLM results of this study reveal a consecutive activation during swallowing of 2 ml of water starting at the PMC, SMA, and bilateral thalamus, continuing on to M1S1, posterior insula, and cerebellum and reaching the brainstem shortly before it subsides. This sequence reflects the preparation and execution stages of swallowing, including the involuntarily controlled pharyngeal phase. An rmANOVA revealed a significant activation over time in M1S1 starting in the left hemisphere and moving on to the right hemisphere. In a DCM model comparison, the model with the highest likelihood is one encompassing the SMA, M1S1, and posterior insula with two different inputs: one to the SMA and the other to M1S1. SMA and M1S1 are connected bidirectionally while M1S1 has a simple connection going to the posterior insula.

REFERENCES

Arce FI, Lee JC, Ross CF, Sessle BJ, Hatsopoulos NG (2013): Directional information from neuronal ensembles in the primate orofacial sensorimotor cortex. Journal of Neurophysiology 110: 1357–1369. doi:10.1152/jn.00144.2013.

Damasio AR (1996): The somatic marker hypothesis and the possible functions of the prefrontal cortex. Philos Trans R Soc London B Biol Sci 351:1413–1420.

Daniels SK (2000): Swallowing apraxia: A disorder of the praxis system? Dysphagia 166:159–166.

Daniels SK, Foundas AL (1997): The role of the insular cortex in dysphagia. Dysphagia 12:146–156.

Dodds W (1989): The physiology of swallowing. Dysphagia 178: 171–178.

Dziewas R, Sörös P, Ishii R, Chau W, Henningsen H, Ringelstein E., Knecht S, Pantev C (2003): Neuroimaging evidence for cortical involvement in the preparation and in the act of swallowing. Neuroimage 20:135–144.

Eickhoff SB, Stephan KE, Mohlberg H, Grefkes C, Fink GR, Amunts K, Zilles K (2005): A new SPM toolbox for combining probabilistic cytoarchitectonic maps and functional imaging data. Neuroimage 25:1325–1335.

Friston KJ, Harrison L, Penny W (2003): Dynamic causal modelling. Neuroimage 19:1273–1302.

Friston KJ, Ashburner JT, Kiebel SJ, Nichols TE, Penny WD (Eds.). (2007): Statistical Parametric Mapping: The Analysis of Functional Brain Images. Functional neuroimaging: Technical (First edition., p. 656). London: Academic Press.

Furlong PL, Hobson AR, Aziz Q, Barnes GR, Singh KD, Hillebrand A, Thompson DG, Hamdy S (2004): Dissociating the spatio-temporal characteristics of cortical neuronal activity associated with human volitional swallowing in the healthy adult brain. Neuroimage 22:1447–1455.

Goyal R, Chaudhury A (2008): Physiology of normal esophageal motility. J Clin Gastroenterol 42:610–619.

Hamdy S, Aziz Q, Rothwell JC, Crone R, Hughes D, Tallis RC, Thompson DG (1997): Explaining oropharyngeal dysphagia after unilateral hemispheric stroke. Lancet 350:686–692.

Hamdy S, Rothwell JC, Brooks DJ, Bailey D, Aziz Q, Thompson DG (1999): Identification of the cerebral loci processing human swallowing with H2(15)O PET activation. J Neurophysiol 81:1917–1926.

Hülsmann E, Erb M, Grodd W (2003): From will to action: Sequential cerebellar contributions to voluntary movement. Neuroimage 20:1485–1492.

Humbert IA, Robbins J (2007): Normal swallowing and functional magnetic resonance imaging: A systematic review. Dysphagia 22:266–275.

Humbert IA, Fitzgerald ME, McLaren DG, Johnson S, Porcaro E, Kosmatka K, Hind J, Robbins J (2009): Neurophysiology of swallowing: Effects of age and bolus type. Neuroimage 44:982–991.

Jean A (2001): Brain stem control of swallowing: Neuronal network and cellular mechanisms. Physiol Rev 81:929–969.

Kern MK, Jaradeh S, Arndorfer RC, Shaker R (2001): Cerebral cortical representation of reflexive and volitional swallowing in humans. Am J Physiol Gastrointest Liver Physiol 280:G354–G360.

Malandraki GA, Sutton BP, Perlman AL, Karampinos DC, Conway C (2009): Neural activation of swallowing and swallowing-related tasks in healthy young adults: An attempt to separate the components of deglutition. Hum Brain Mapp 30:3209–3226.

Malandraki G, Sutton B, Perlman A, Karampinos D (2010): Age-related differences in laterality of cortical activations in swallowing. Dysphagia 25:238–249.

Maldjian JA, Laurienti PJ, Kraft RA, Burdette JH (2003): An automated method for neuroanatomic and cytoarchitectonic atlas-based interrogation of fMRI data sets. Neuroimage 19:1233–1239.

Martin RE, Goodyear BG, Gati JS, Menon RS (2001): Cerebral cortical representation of automatic and volitional swallowing in humans. J Neurophysiol 85:938–950.

Mazaika PK, Whitfield-Gabrieli S, Reiss A, Glover G (2009): Artifact Repair for fMRI Data from High Motion Clinical Subjects. Poster presented at the Human Brain Mapping Conference in San Francisco, CA, USA.

Michou E, Hamdy S (2009): Cortical input in control of swallowing. Curr Opin Otolaryngol Head Neck Surg 17:166–171.

Miezin FM, Maccotta L, Ollinger JM, Petersen SE, Buckner RL (2000): Characterizing the hemodynamic response: effects of presentation rate, sampling procedure, and the possibility of ordering brain activity based on relative timing. NeuroImage 11(6 Pt 1):735–759. doi:10.1006/nimg.2000.0568.

Mihai PG, von Bohlen Und Halbach O, Lotze M (2013): Differentiation of cerebral representation of occlusion and swallowing with fMRI. Am J Physiol Gastrointest Liver Physiol 304:847–854.

Mosier K, Bereznaya I (2001): Parallel cortical networks for volitional control of swallowing in humans. Exp Brain Res 140:280–289.

Mosier KM, Liu WC, Maldjian JA, Shah R, Modi B (1999): Lateralization of cortical function in swallowing: A functional MR imaging study. AJNR Am J Neuroradiol 20:1520–1526.

Ramsey GH, Watson JS, Gramiak R, Weinberg SA (1955): Cinefluorographic analysis of the mechanism of swallowing. Radiology 64(4):498–518.

Reimers-Neils L (1994): Viscosity effects on EMG activity in normal swallow. Dysphagia 106:101–106.

Riecker A, Gastl R, Kühnlein P, Kassubek J, Prosiegel M (2009): Dysphagia due to unilateral infarction in the vascular territory of the anterior insula. Dysphagia 24:114–118.

Robbins J (1993): Swallowing after unilateral stroke of the cerebral cortex. Arch Phys Med Rehabil 74:1295–1300.

Sörös P, Inamoto Y, Martin RE (2009): Functional brain imaging of swallowing: An activation likelihood estimation meta-analysis. Hum Brain Mapp 30:2426–2439.

Stephan KE, Penny WD, Daunizeau J, Moran RJ, Friston KJ (2009): Bayesian model selection for group studies. Neuroimage 46: 1004–1017.

Stueve D (2006): Management of pediatric radiation dose using Philips fluoroscopy systems DoseWise: Perfect image, perfect sense. Pediatr Radiol 36(Suppl 2):216–220.

Teismann IK, Dziewas R, Steinstraeter O, Pantev C (2009): Time-dependent hemispheric shift of the cortical control of volitional swallowing. Hum Brain Mapp 30:92–100.

Toogood JA, Barr AM, Stevens TK, Gati JS, Menon RS, Martin RE (2005): Discrete functional contributions of cerebral cortical foci in voluntary swallowing: A fMRI "Go, No-Go" study. Exp Brain Res 161:81–90.